JVSTA
JOURNAL OF VACUUM SCIENCE AND TECHNOLOGY A

Rotational dynamics of desorption and inelastic scattering for the NO/Pt(111) system

D. C. Jacobs, K. W. Kolasinski, R. J. Madix, and R. N. Zare

Citation: J. Vac. Sci. Technol. A **7**, 1871 (1989); doi: 10.1116/1.576019
View online: http://dx.doi.org/10.1116/1.576019
View Table of Contents: http://avspublications.org/resource/1/JVTAD6/v7/i3
Published by the AVS: Science & Technology of Materials, Interfaces, and Processing

Rotational dynamics of desorption and inelastic scattering for the NO/Pt(111) system

D. C. Jacobs,[a] K. W. Kolasinski, R. J. Madix,[b] and R. N. Zare
Department of Chemistry, Stanford University, Stanford, California 94305

(Received 23 August 1988; accepted 12 September 1988)

The rotational population and alignment distributions of NO are measured subsequent to the molecule's interaction with a clean Pt(111) surface. Two distinct dynamical regimes of trapping/desorption and inelastic scattering are studied over the temperature range 375–550 K. For the case of molecular desorption, molecules which desorb with a large amount of angular momentum ($J > 12.5$) prefer to rotate in the plane of the surface. Those molecules which scatter from the surface show the opposite preference for rotational alignment, i.e., they preferentially rotate in a plane perpendicular to the surface. The non-Boltzmann rotational distribution reveals that a large fraction of the scattered molecules contain more energy in rotation than initially exists as total energy in the beam. This observation indicates the important role of surface vibration to rotational energy transfer in this system. A quasiclassical stochastic trajectory model is able to account for much of the observed phenomena.

I. INTRODUCTION

The details of a molecule–surface potential are realized through a battery of complementary techniques. Standard surface spectroscopies [e.g., low-energy electron diffraction (LEED), ultraviolet photoelectron spectroscopy (UPS), x-ray photoelectron spectroscopy (XPS), electron energy-loss spectroscopy (EELS), infrared reflection–absorption spectroscopy (IRAS), surface enhanced Raman spectroscopy (SERS), electron stimulated desorption ion angular distribution (ESDIAD), surface extended x-ray absorption fine structure (SEXAFS), etc.] probe the distinguishing features at the bottom, or equilibrium position, of the potential well. In contrast, dynamical measurements of fundamental surface processes (e.g., direct inelastic scattering, adsorption, activated dissociation, diffusion, desorption, etc.) reveal information about the top of the potential well near the transition state. The present study examines the rotational dynamics of NO as it escapes from a Pt(111) surface.

The chemistry of NO on Pt(111) has been studied by many groups. NO is believed to occupy a bridge site at low coverage, an atop site at moderate coverages, and an elusive disordered site at coverages above 0.25 monolayers (ML).[1–4] The coverage-dependent binding energy varies from 100 to 140 kJ/mol.[5] The initial sticking probability lies between 0.85 and 0.90, independent of surface temperature.[6,7] Dissociation is believed to take place only at defect sites on the surface.[5,6] Scattering studies have found that the accommodation coefficients for translational and vibrational energy are close to unity and are fairly invariant to surface temperature.[8] However, the measured rotational temperature of the scattered distribution appears to deviate more strongly from the surface temperature and reaches an asymptotic value of 450 K.[9–14] Rotational alignment in the scattered and desorbed NO has not been observed for Pt(111).[11,14]

This paper discusses the rotational dynamics of NO from Pt(111) for two distinct regimes: trapping/desorption and inelastic scattering. Inelastic scattering refers to a collision of short duration (one or a few bounces) between the molecule and surface. The molecule scatters with an energy distribution characteristic of both the molecule's initial conditions and the nature of the surface. Trapping/desorption involves a relatively long surface residence time in which the molecule loses "memory" of its initial conditions. In this latter case, the desorbed molecule's energy distribution is characterized solely by the conditions of the surface and the molecule–surface potential.

Our probe of the system is the measure of rotational population and alignment distributions. Population refers to the relative number of molecules in a particular rotational state while alignment concerns the spatial distribution of the rotational angular momentum vector. Figure 1 shows two limiting cases of rotational alignment. In the lab, we distinguish between these cases by determining the value of the quadrupole moment $A_0^{(2)}(J)$. It is simply a number which ranges from -1 (pure "cartwheel" motion) to $+2$ (pure "helicopter" motion), where a value of 0 implies that there is no preferential alignment.[15]

Additionally, we report the predictions of a simple trajectory model which has been applied to this system.[16] The proposed model is far less computationally intensive than the generalized Langevin equation (GLE) approach because the model has a simplified description of surface motion. However, the current model does use a similar realistic molecule–surface potential to the one employed in the GLE calculations. In the case of trapping/desorption, the model

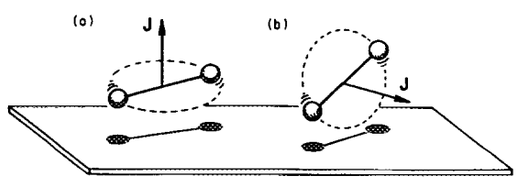

FIG. 1. Rotational alignment relative to the surface plane. The helicopter motion (a) is preferred for $A_0^{(2)} > 0$; the cartwheel motion (b) is favored for $A_0^{(2)} < 0$.

 0734-2101/89/031871-07$01.00

accurately describes the observed dependence of rotational alignment on rotational quantum number. For the inelastic scattering regime, the model successfully reproduces the degree of rotational excitation and qualitatively accounts for the observed rotational alignment. The experimental data, along with the predictions of the model, provide a dynamical picture of the interaction of nitric oxide with a clean Pt(111) surface.

II. EXPERIMENTAL

The experimental configuration shown in Fig. 2 is described in detail elsewhere.[17] Prior to the experiment, the Pt(111) sample is cleaned by oxidation and annealing treatments. Both LEED and Auger suface diagnostics are used to insure surface order and cleanliness. A differentially pumped molecular beam (neat expansion, 50 psi stagnation pressure, 100-μs temporal width) provides the Pt surface with 0.066L pulses of NO at 10 Hz. A sizable fraction of the incident pulse of NO scatters from the surface. The remainder traps on the surface and desorbs later.

A pulsed Nd:yttrium–aluminum–garnet (YAG) pumped dye laser system provides the means for state-selective detection of the nascent molecules. The 6-ns laser pulse (225-nm wavelength) passes 2 mm above the Pt crystal face and excites a portion of those molecules that have interacted with the surface. The laser spectroscopy employed for this purpose is $1 + 1$ resonance enhanced multiphoton ionization (REMPI) spectroscopy.[15,18] Here, the linearly polarized laser beam selectively ionizes those NO molecules that occupy a particular rotational level of the ground vibrational state. The choice of rotational levels is selected by tuning the laser wavelength. The measure of alignment in a particular rotational level is calculated from the laser polarization dependence of the REMPI in signal.[15,17,18] The ions resulting from the REMPI excitation are accelerated through a time-of-flight tube and collected by a charged particle multiplier (CEMA multichannel plates). The ion signal is digitized by a CAMAC charge sensitive gated integrator and passed to the computer for storage. This dose/detect cycle is repeated at 10 Hz while the laser wavelength is scanned. Additionally, the light's plane of polarization is alternated between two orthogonal directions. Magnetic fields in the laser interaction region are minimized through the use of external Helmholtz coils and by turning off the heater filament current during the laser pulse.

The experiments are peformed with the molecular beam at normal incidence to the surface. Detection occurs over a 70° acceptance angle centered about the surface normal. The dynamical regimes of direct inelastic scattering and trapping/desorption are differentiated according to their characteristic surface residence times. The residence time for direct inelastic scattering is infinitesimal on the microsecond time scale of the molecular-beam pulse. However, the

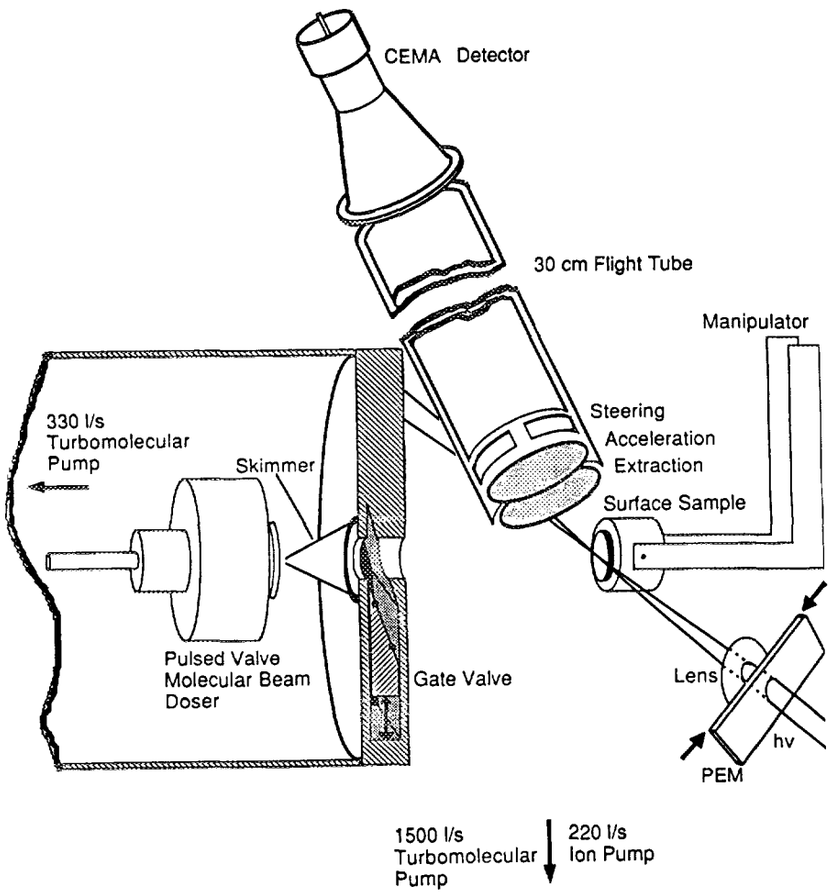

FIG. 2. Experimental apparatus. A differentially pumped pulsed valve doses the Pt(111) crystal. Laser radiation is focused 2 mm above the surface. Ions produced in the REMPI process are accelerated through the time-of-flight tube and collected by the CEMA charged particle multiplier. The crystal can be rotated in order to face LEED and Auger diagnostics. Not shown are Helmholtz coils which reduce stray magnetic fields.

trapped state, at low coverage, will exhibit a half-life on the surface which is inversely proportional to the desorption rate constant. For our temperature regime, the half-life is estimated to be 2–2000 ms. Synchronizing the laser to fire during the nozzle pulse discriminates in favor of those molecules which have inelastically scattered. Conversely, firing the laser 200 μs after the 90-μs nozzle pulse precludes inelastic scattering contributions and permits only detection of those molecules which have been trapped and subsequently desorbed. The surface coverage at which these experiments are performed is estimated to be $< 3\%$ of a monolayer.[17]

III. TRAJECTORY MODEL

A quasiclassical stochastic trajectory method was developed to model the dynamics of inelastic scattering and trapping/desorption mechanisms on single-crystal surfaces. The model is appealing because the comprehensive information revealed by a trajectory analysis is realized with the use of conventional computational facilities (e.g., a VAX) rather than a supercomputer. Although the model is described in detail elsewhere,[16] we briefly summarize its constructs here.

Newton's equations of motion are integrated for a rigid rotor interacting with a slab of 19 surface atoms (see Fig. 3).

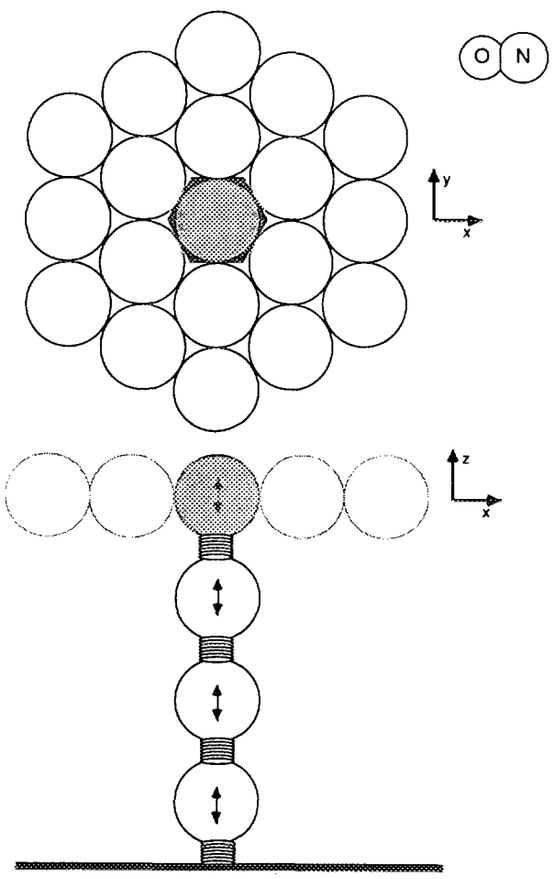

FIG. 3. Schematic of Pt(111) slab used in trajectory calculations. (a) Surface planar and (b) cross-sectional views of the slab show the 18 static surface atoms, the one mobile surface atom, and the three mobile subsurface atoms. The hexagonal shaded area defines the active zone which is defined relative to the position of the NO molecule (drawn to scale).

Because the predominant mechanism for momentum transfer between a molecule and a surface is the out-of-plane motion of the nearest surface atom, we limit the model's treatment of surface motion to precisely that. The surface atom which is closest to the molecule is identified as the "active surface atom." The model permits it to translate only along the surface normal. The active surface atom, in turn, is coupled to three subsurface mobile atoms (ghost atoms) through a linear harmonic chain. The chain is terminated by a connection to a stationary substrate block. Together, the four mobile Pt atoms simulate a microcanonical heat bath. When the molecule diffuses along the surface and leaves its current "active zone" (as indicated by the shaded area in Fig. 3), the model switches the substrate so that the molecule finds itself entering a new active zone surrounded again by 18 stationary surface atoms. Throughout the entire trajectory, the active zone tracks the molecule.

The surface molecule potential is composed of pairwise interactions summed over all 19 surface atoms. The functional form of the pairwise interaction is taken from the empirical potential developed by Muhlhausen, Williams, and Tully.[19] These authors optimized the potential's functional form in order that it might simulate the bond energies, lengths, angles, and vibrational frequencies measured previously for the NO/Pt(111) system. The potential energy hypersurface has a strong dependence on molecular orientation and favors linear bonding through the nitrogen atom via an atop site.

All trajectories start with the NO center of mass located 6 Å from the surface. The positions of the 18 stationary surface atoms match the equilibrium positions of the Pt(111) face. The initial orientation of the internuclear axis, the incident velocity, the two-dimensional surface impact parameter, and the momenta and positions of the four mobile surface atoms are chosen stochastically. They are selected in a manner which simulates the experimental conditions of a supersonic NO beam striking a Pt(111) surface at temperature T_s. The equations of motion are numerically integrated with a $\sim$1-fs time interval. The trajectory is terminated when either the molecule scatters beyond 6 Å or the trajectory has run for as long as 6 ps without the molecule escaping from the surface (at which time the molecule is considered trapped). The desorption dynamics are inferred from detailed balance arguments applied to the fraction of trajectories that are trapped.[20]

IV. RESULTS

A. Trapping/desorption

The rotational alignment distribution of NO is measured subsequent to the molecule's desorption from a Pt(111) surface at 553 K. The laser is synchronized to fire 200 μs after the end of the nozzle pulse. The surface temperature is chosen from a relatively narrow range of temperatures at which the surface residence time is on the order of the laser-nozzle delay. The laser is tuned to a particular rotational transition and ions are collected for 1000–10 000 laser shots at alternating laser polarization directions. The polarization dependence of a given rotational transition is directly related to the

quadrupole moment of the rotational alignment distribution.

A summary represenation of the data, reported elsewhere,[21] is shown in Fig. 4. The shaded portion of the figure corresponds to the experimental data, including error bars. For $J < 12.5$, there appears to be little to no rotational alignment. However, molecules with $J > 12.5$ show increasing values of the quadrupole moment. The maximum measured quadrupole moment ($+0.15$) implies that 1.2–1.5 times as many molecules desorb with their plane of rotation resembling that of a helicopter as those resembling a cartwheel motion[22] (see Fig. 1).

The trajectory model predicts a rotational alignment dependence for trapping. Through detailed balance, this result is converted into predictions of the rotational alignment associated with desorption (see Fig. 4). These values of the quadrupole moment for desorption are plotted for both flux-sensitive and number density-sensitive detection.[23] The model's results are in excellent agreement with the experimental data.

B. Inelastic scattering

The laser is fired synchronously with the rising edge of the nozzle pulse. For the temperature range examined, this discriminates in favor of those molecules that have bounced once or a few times on the surface. Scattering of the 9-kJ/mol molecular beam is performed at five different surface temperatures between 375 and 475 K. The laser is scanned at a rate which permits, for each rotational line profile, ~50 shots of signal averaging for each of the two orthogonal laser polarizations. The REMPI line intensities are then reduced to both rotational population and alignment distributions. Rotational population distributions are often presented in the form of a Boltzmann plot. Here, the natural logarithm of the relative population is plotted against the internal energy for each rotational level. For the case of a thermal distribution, the corresponding Boltzmann plot would yield a straight line, where the slope of the line is inversely proportional to the rotational temperature.

Figure 5 shows a Boltzmann plot of the inelastically scattered component of NO from Pt(111) at 450 K. The data do not fall on a single line. In fact there appears to be three somewhat linear portions to the Boltzmann plot. These are marked with temperatures only to show the relative amount of rotational excitation in each of these three regions. The temperatures are not meant to imply that the rotational distribution is "thermal" or even "trimodal." The low J region of the plot is biased by an experimental artifact—detection of the incident beam. Normal incidence/normal detection is sensitive to both incoming and outgoing molecules. However, the incident neat beam is rotationally cold (measured to be 40 K) and will only interfere with the populations measured for the lowest rotational levels ($J < 7.5$). The vertical dashed line at 690 cm^{-1} represents the total energy of the incident supersonic beam. In the rigid surface limit, rotational excitation beyond this energy would be strictly forbidden. However, the experiment reveals that a significant fraction of the molecules escape the surface with more energy in rotation than they initially possessed as total energy in the incident beam.

The rotational alignment distribution for inelastically scattered NO from Pt(111) at 450 K is shown in the inset of Fig. 5. For $J < 10.5$ there is no appreciable alignment. Of course interference of the incident molecular beam will dilute the observable alignment. Beyond $J = 10.5$ there is a steady rise in the quadrupole moment until it peaks around $J = 25.5$. This implies that scattered molecules prefer to rotate in a plane normal to the surface, i.e., to undergo cartwheel motion (see Fig. 1). This preference has been seen for the scattering of NO[24–26] and N_2 (Refs. 27–29) from Ag(111). Beyond $J = 25.5$, the alignment for NO/Pt(111) appears to decrease. However, these high-J data are associat-

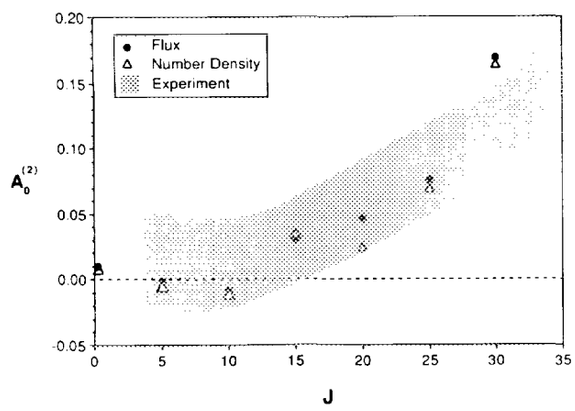

FIG. 4. The quadrupole moment of the rotational alignment distribution $A_0^{(2)}(J)$ for NO desorption at 553 K. The data, including error bars, are represented by the shaded region. The solid circles and open triangles correspond to the trajectory calculations where the alignment is measured with flux-sensitive detection and number density-sensitive detection, respectively.

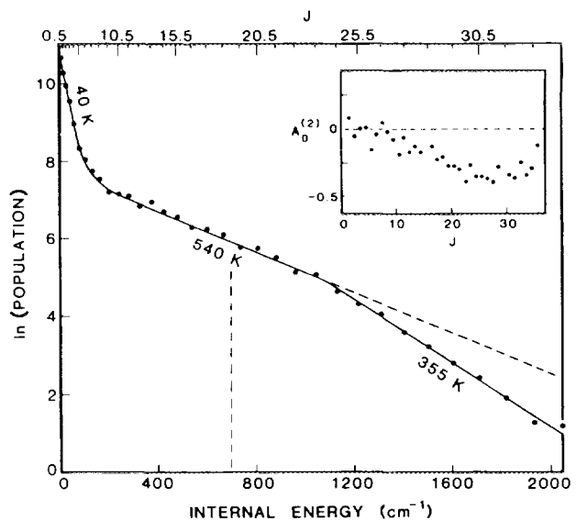

FIG. 5. Inelastic scattering of NO from Pt(111) at 450 K. A Boltzmann plot of the population distribution reveals three linear regions, described by the listed rotational temperatures. The vertical dashed line represents the total energy in the incident molecular beam. The inset shows the corresponding rotational alignment distribution $A_0^{(2)}(J)$.

ed with larger error bars, and thus a quantitative determination of the decrease in alignment cannot be made at this time.

Figure 6 summarizes the inelastic results at five different surface temperatures and compares them to predictions from the trajectory model. For clarity, the experimental results reported elsewhere[17] are represented by curves that pass through the data points. The surface temperature of each data set is indicated on the figure. The experimental curves are normalized to the population in $J = 0.5$. Because the population in this state is due primarily to the incident beam, this normalization procedure scales the data to the incident beam intensity. Trajectory calculations simulate inelastic scattering at two surface temperatures (shown as open and solid circles). The theoretical predictions lack the low J interference found in the experiment, and thus we scale them according to their populations in the intermediate J region. The population data indicate that the amount of rotational excitation in the scattered distribution increases with increasing surface temperature. The model's predictions reflect this same trend. The population data at 375 K may represent scattering from a partially NO covered surface. This would have the effect of dramatically diminishing both the degree of rotational excitation and the amount of in-plane scattering.

The corresponding quadrupole moment $A_0^{(2)}(J)$ is plotted in the inset of Fig. 6. The data appear to be relatively independent of temperature within the experimental error. The model's prediction of the rotational alignment deviates from experiment at both low and high J. Comparison of theory and experiment at low J is difficult because interference from the incident beam will reduce the observable rotational alignment. However, the discrepancy between theory and experiment at high J is more serious.

V. DISCUSSION

These experiments mark the first observation of rotational alignment in desorption. They also represent the first study of inelastic scattering in which rotational states up to three times more energetic than the incident beam energy are examined for alignment. The opposite preference in rotational alignment measured for desorption and inelastic scattering suggests that these two processes have very different dynamical pathways on the same potential energy surface.

The rotational alignment measured for desorption implies that molecules escaping the surface with large amounts of rotational angular momenta prefer to rotate in the plane of the surface. This surprising preference for helicopter motion is inconsistent with the simple desorption picture of a direct transition from the known low-temperature equilibrium geometry (NO bound normal to the surface) to a gas-phase free rotor. Our measurements are sensitive to the last few interactions the molecule makes with the surface before desorbing, i.e., the nature of the molecule–surface potential near the transition state. The results suggest that the molecule is rotating on the surface immediately prior to desorption. Rotation of an adsorbed molecule in the plane of the surface is less hindered than rotation in a plane normal to the surface. This implies that there exists a higher density of rotational states associated with helicopter motion on the surface than those associated with a cartwheel motion. Thermal population of these surface hindered-rotor states[30] followed by cleaveage of the molecule–surface bond will leave the desorbed molecule with a preference toward helicopter motion (Fig. 7).

The model predicts a rotational alignment dependence for adsorption of molecules in high J. This can be attributed to a dynamical effect: rotational angular momentum is more effi-

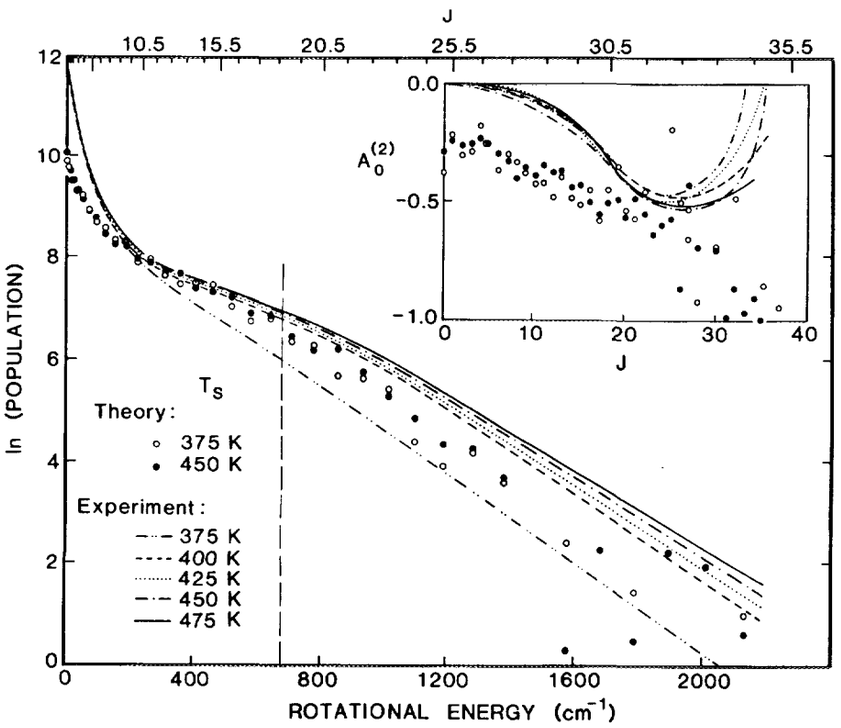

FIG. 6. Inelastic scattering distributions of NO from Pt(111). The Boltzmann plots and alignment distributions (inset) are shown for experiment (curves) and theory (solid and open circles) at the listed surface temperatures.

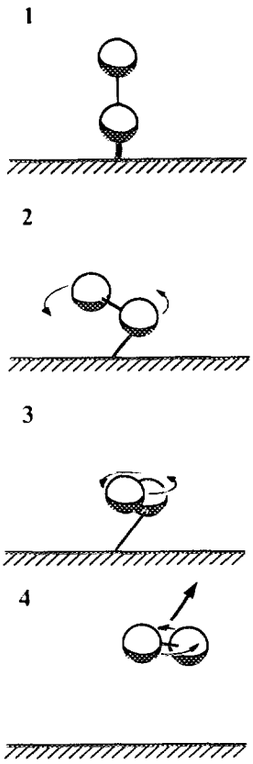

FIG. 7. Proposed mechanism for desorption into high-J rotational states. Frame 1 shows the low-temperature equilibrium geometry for NO on Pt(111). Rotation on the surface is less hindered in the plane parallel to the surface. Frames 2 and 3 show a rotationally excited species on the surface. Cleavage of the chemisorption bond (frame 4) leads to a preference for helicopter motion in the escaping molecule.

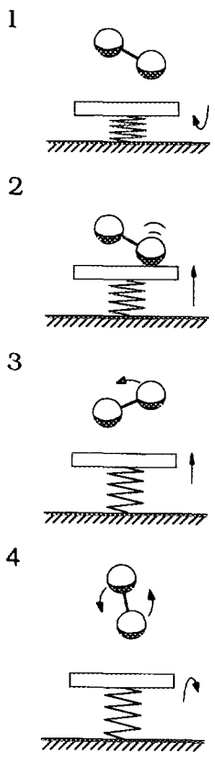

FIG. 8. Proposed mechanism for inelastic scattering into high-J rotational states. A vibrating surface atom is sketched as a block on a spring. Frame 1 shows the molecule accelerating into the surface. The collision (frame 2) occurs while the molecule has a tilted orientation with respect to the surface normal, and the surface atom is moving away from the bulk. Incident translational energy and surface vibrational energy are converted into rotational energy in the outgoing molecule. In frames 3 and 4, the molecule escapes the potential well.

ciently converted to linear momentum along the surface normal for molecules rotating in a plane perpendicular to the surface (cartwheel motion) than for molecules rotating in a plane parallel to the surface (helicopter motion). It is normal linear momentum that assists the molecule in escaping the attractive well. Hence, molecules striking the surface with rotational motion resembling that of a cartwheel have a lower chance of trapping than those that approach with a helicopter motion. This result is consistent with the preference measured for desorption.

The Boltzmann plots of Figs. 5 and 6 reveal the presence of a surface vibration-to-rotational energy transfer mechanism in inelastic scattering. In general, if the surface atom closest to the molecule is translating out of the bulk during the surface collision, then the molecule will gain translation and/or rotational energy (see Fig. 8). The degree of rotational excitation in the scattered distribution increases with increasing surface temperature. Although significant surface-to-rotational energy transfer is responsible for populating states with rotational energy exceeding the beam energy, rotational alignment is created in these states and is preserved in the final distribution.

The model predicts a similar amount of rotational excitation as that observed experimentally. Additionally, the trajectories reveal that rotational excitation increases with the number of bounces the molecule makes with the surface before escaping. Only 60% of the inelastic scattering trajectories escape the surface after one bounce. The trajectories also indicate a decrease in the average rotational alignment with an increase in the number of bounces. Together this may explain the measured falloff in rotational alignment with increasing J. The discrepancy between theory and experiment at high J may be caused by an underestimation of the fraction of multiple bounce trajectories contributing to the populations in the highest rotational states.

Rotational population and alignment distributions have provided a sensitive probe of gas–surface dynamics. In particular, such studies reveal information about energy transfer processes at surfaces and anisotropies in the molecule–surface potential near the transition state.

ACKNOWLEDGMENTS

This work was supported by the Office of Naval Research (N00014-87-K-00265). We gratefully acknowledge the assistance of Stacey F. Shane.

[a] Present address: Department of Chemistry, University of Notre Dame, Notre Dame, IN 46556.
[b] Joint appointment with Chemical Engineering Department.

[1] H. Ibach and S. Lehwald, Surf. Sci. **76**, 1 (1978).
[2] J. L. Gland and B. A. Sexton, Surf. Sci. **94**, 355 (1980).
[3] B. E. Hayden, Surf. Sci. **131**, 419 (1983).
[4] M. Kiskinova, G. Pirug, and H. P. Bonzel, Surf. Sci. **136**, 285 (1984).
[5] R. J. Gorte, L. D. Schmidt, and J. L. Gland, Surf. Sci. **109**, 367 (1981).
[6] J. A. Serri, M. J. Cardillo, and G. E. Becker, J. Chem. Phys. **77**, 2175 (1982).
[7] C. Campbell, G. Ertl, and J. Segner, Surf. Sci. **115**, 309 (1982).
[8] W. L. Guthrie, T. -H. Lin, S. T. Ceyer, and G. A. Somorjai, J. Chem. Phys. **76**, 6398 (1982).
[9] F. Frenkel, J. Häger, W. Krieger, H. Walther, C. Campbell, *et al.*, Phys. Rev. Lett. **46**, 152 (1981).
[10] M. Asscher, W. Guthrie, T. Lin, and G. Somorjai, Phys. Rev. Lett. **49**, 76 (1982).
[11] J. Segner, H. Robota, W. Vielhaber, G. Ertl, F. Frenkel *et al.*, Surf. Sci. **131**, 273 (1983).

[12]M. Asscher, W. Guthrie, T. Lin, and G. Somorjai, J. Chem. Phys. **78**, 6992 (1983).
[13]D. S. King, D. A. Mantell, and R. R. Cavanagh, J. Chem. Phys. **82**, 1046 (1985).
[14]D. A. Mantell, R. R. Cavanagh, and D. S. King, J. Chem. Phys. **84**, 5131 (1986).
[15]D. C. Jacobs, R. J. Madix, and R. N. Zare, J. Chem. Phys. **85**, 5469 (1986).
[16]D. C. Jacobs and R. N. Zare, J. Chem. Phys. (submitted).
[17]D. C. Jacobs, K. W. Kolasinski, S. F. Shane, and R. N. Zare, J. Chem. Phys. (submitted).
[18]D. C. Jacobs and R. N. Zare, J. Chem. Phys. **85**, 5457 (1986).
[19]C. W. Muhlhausen, L. R. Williams, and J. C. Tully, J. Chem. Phys. **83**, 2594 (1985).
[20]For the case of simulating trapping/desorption, the total angular momentum of the incident molecule is preselected so that the dynamics of a single rotational quantum state can be examined. However, the translational energy distribution is Maxwellian at the surface temperature T_s with an incident angular distribution of cos θ.
[21]D. C. Jacobs, K. W. Kolasinski, R. J. Madix, and R. N. Zare, J. Chem. Phys. **87**, 5038 (1987).
[22]The limiting values of this range assume that the rotational alignment distribution is best described by either an ellipsoid or a function, which contains a linear combination of $\cos^2\theta$ and $\sin^2\theta$, respectively. The trajectory calculations suggest that the latter function provides a more accurate description of the distribution. In any case, these two functional forms probably represent the limiting cases for the alignment distribution.
[23]Our experimental configuration is sensitive to the number density of molecules in a particular rotational state. The calculations suggest that the velocity of a desorbing molecule is relatively uncorrelated with its rotational alignment. Hence, the two forms of detection sensitivity yield similar results.
[24]A. Luntz, A. Kleyn, and D. Auerbach, Phys. Rev. B **25**, 4273 (1982).
[25]A. Kleyn, A. Luntz, and D. Auerbach, Surf. Sci. **117**, 33 (1983).
[26]A. Kleyn, A. Luntz, and D. Auerbach, Surf. Sci. **152**, 99 (1985).
[27]G. O. Sitz, A. C. Kummel, and R. N. Zare, J. Vac. Sci. Technol. A **5**, 513 (1987).
[28]G. O. Sitz, A. C. Kummel, and R. N. Zare, J. Chem. Phys. **87**, 3247 (1987).
[29]G. O. Sitz, A. C. Kummel, and R. N. Zare, J. Chem. Phys. **89**, 2558 (1988).
[30]Hindered rotation of chemisorbed molecules has been directly observed. For example, see M. D. Alvey, J. T. Yates, Jr., and K. J. Uram, J. Chem. Phys. **87**, 7221 (1987).